# Oviductal Retention of Embryos in Female Mice Lacking Estrogen Receptor α in the Isthmus and the Uterus

Gerardo G.B. Herrera,[1,*] Sydney L. Lierz,[2,*] Emily A. Harris,[1] Lauren J. Donoghue,[2] Sylvia C. Hewitt,[2] Karina F. Rodriguez,[2] Wendy N. Jefferson,[2] John P. Lydon,[3] Francesco J. DeMayo,[2] Carmen J. Williams,[2] Kenneth S. Korach,[2] and Wipawee Winuthayanon[1,2]

[1]School of Molecular Biosciences, Center for Reproductive Biology, College of Veterinary Medicine, Washington State University, Pullman, Washington, 99164 US; [2]Reproductive and Developmental Biology Laboratory, National Institute of Environmental Health Sciences, National Institutes of Health (NIH/NIEHS), Department of Health and Human Services, Research Triangle Park, North Carolina, 27709 US; and [3]Department of Molecular and Cellular Biology, Baylor College of Medicine, Houston, Texas, US.

**ORCiD numbers:** 0000-0001-7713-0805 (S. C. Hewitt); 0000-0002-9480-7336 (F. J. DeMayo); 0000-0001-6440-7086 (C. J. Williams); 0000-0002-7765-418X (K. S. Korach); 0000-0002-5196-8471 (W. Winuthayanon).

Estrogen receptor α (ESR1; encoded by *Esr1*) is a crucial nuclear transcription factor for female reproduction and is expressed throughout the female reproductive tract. To assess the function of ESR1 in reproductive tissues without confounding effects from a potential developmental defect arising from global deletion of ESR1, we generated a mouse model in which *Esr1* was specifically ablated during postnatal development. To accomplish this, a progesterone receptor Cre line ($Pgr^{Cre}$) was bred with $Esr1^{f/f}$ mice to create conditional knockout of *Esr1* in reproductive tissues (called $Pgr^{Cre}Esr1$KO mice) beginning around 6 days after birth. In the $Pgr^{Cre}Esr1$KO oviduct, ESR1 was most efficiently ablated in the isthmic region. We found that at 3.5 days post coitus (dpc), embryos were retrieved from the uterus in control littermates while all embryos were retained in the $Pgr^{Cre}Esr1$KO oviduct. Additionally, serum progesterone ($P_4$) levels were significantly lower in $Pgr^{Cre}Esr1$KO compared to controls at 3.5 dpc. This finding suggests that expression of ESR1 in the isthmus and normal $P_4$ levels allow for successful embryo transport from the oviduct to the uterus. Therefore, alterations in oviductal isthmus ESR1 signaling and circulating $P_4$ levels could be related to female infertility conditions such as tubal pregnancy. **(*Endocrinology* 161: 1–12, 2020)**

**Key Terms:** embryo transport, estrogen receptor α, oviduct, pituitary gland, uterus

Estrogens, which are sex steroid hormones, carry out their physiological action through estrogen receptors (encoded by *Esr* genes). Global estrogen receptor α (ESR1) knockout mice ($Esr1^{-/-}$, originally called αERKO) exhibit female infertility due to an ovulatory defect and to a lack of estrogen-induced uterine responsiveness (1). In humans, loss of functional ESR1 or mutation in the ESR1 ligand binding domain recapitulate the phenotypes found in the αERKO mouse model (2, 3). Global loss of estrogen receptor β or *Esr2* ($Esr2^{-/-}$) in mice causes reduced folliculogenesis but not complete sterility (4). As such, in this study, we focused on the evaluation of estrogen action in the female reproductive tract through ESR1.

The αERKO mouse model provided a robust starting point to determine the functional requirement for ESR1 in reproductive physiology. However, there was a major

ISSN Online 1945-7170

Accepted 16 December 2019.
First Published Online 28 December 2019.
Corrected and Typeset 12 February 2020.

*Co-first authors, equal contribution

concern regarding the use of this αERKO model—the potential developmental loss of tissue responsiveness due to lack of *Esr1* during embryonic development in utero (1). To circumvent this concern, we recently generated a mouse model in which *Esr1* was conditionally ablated in the uterus, oviduct, and pituitary gland postnatally, by the breeding of $Esr1^{f/f}$ (5) with progesterone receptor (PGR)-driven Cre expression ($Pgr^{Cre}$) mice (6). In mice, the expression of PGRs begins approximately at postnatal day 6 in the uterine epithelial cells (6, 7). Then, the expression gradually increases in stromal cells (or fibroblasts) and muscle cell layers after the first ovarian cycle. In the oviduct, the activity of $Pgr^{Cre}$ is observed in the isthmic region, but not the infundibulum or ampullary regions (6, 8). Therefore, this $Pgr^{Cre/+}/Esr1^{f/f}$ mouse model (hereafter $Pgr^{Cre}$*Esr1*KO) allows for the evaluation of ESR1 function in the oviduct, uterus, and pituitary gland, without potential developmental defects in contrast to the αERKO model in which *Esr1* is deleted in gametes and thus lacks ESR1 at all stages of development.

In addition, αERKO females do not ovulate normally, hindering our capability to evaluate the effect of estrogen signaling on the egg/embryo development within the female reproductive tract. Based on these features, the $Pgr^{Cre}$*Esr1*KO mouse is an appropriate model for evaluation and truly reflects the function of ESR1 in mammalian female reproduction. Herein, we assessed the requirement for ESR1 in regulating oviductal function during embryo development and transport, serum levels of luteinizing hormone (LH), 17β-estradiol ($E_2$), and progesterone ($P_4$), morphology of the ovary, and uterine responsiveness to estrogen using the $Pgr^{Cre}$*Esr1*KO mouse model.

## Materials and Methods

### Animals

All animals were maintained at the National Institute of Environmental Health Sciences (NIEHS) and were handled according to Animal Care and Use Committee guidelines. The oviductal and uterine *Esr1* knockout mouse model was generated by breeding $Pgr^{Cre/+}$ (6) with $Esr1^{f/f}$ animals (5). For most studies, mice used were from a colony on a C57Bl6/J background. For evaluating serum $E_2$ and $P_4$ at 3.5 days post coitus (dpc), the mice were from a colony that had been back crossed onto FVBN. The conditional knockout females ($Pgr^{Cre}$*Esr1*KO) and $Esr1^{f/f}$ control littermates were used in the experiments. Genotyping protocols for $Esr1^{f/f}$ and $Pgr^{Cre}$ were performed as previously described (5, 6). The genotype of each mouse was validated and confirmed using ESR1 immunohistochemical analysis in the uterine sample using the protocol described in the following text. The oviduct, ovaries, and uterus were collected from adult $Pgr^{Cre}$*Esr1*KO and $Esr1^{f/f}$ females for histological analysis. Tissues were fixed in 10% formalin and processed for standard hematoxylin and eosin (H&E) staining. The estrous cycle was evaluated using cytological analysis from vaginal smear for 10 days (ranging from 47 to 64 days old) as previously described ($n$ = 7–10 mice/genotype) (9). The pituitary gland and serum were collected from random stages of estrous cycle ovarian intact 7- to 18-week-old females at 9:00 AM to 11:00 AM for protein expression analysis and LH levels, respectively. The LH assay was performed using 20 μL of serum from each animal as previously described ($n$ = 20–25 mice/genotype) (5). For the breeding trial, females were housed with wild-type (WT) male proven breeders for 6 consecutive months ($n$ = 4–6 mice/genotype). The number of pups per litter per dam and litter interval were recorded.

### Western blot analysis

Protein was extracted and analyzed as described previously with slight modifications (10). Briefly, a total of 25 μg protein was used for the experiment. Nitrocellulose blot was probed with rabbit anti ESR1 (11) (SC542, Santa Cruz Biotechnology, Inc., Santa Cruz, CA, US) listed in Antibody Table 1 at a dilution of 1:650 in 5% nonfat dry milk in tris-buffered saline containing 0.01% Tween 20 (TBST) ($n$ = *3* mice/genotype). The monoclonal anti β-actin (12) (A2228, Sigma, St Louis, MO, US) was used at a dilution of 1:2000 in 5% milk TBST ($n$ = 3 mice/genotype). Goat anti-rabbit IRDye 800 CW and goat anti-mouse IRDye 680 RD secondary antibodies (Li-COR Biotechnology, Lincoln, NE, US) were used for detection of ESR1 and β-actin, respectively at a dilution of 1:50 000 in 5% milk TBST. Protein expression was visualized using Odyssey FC imaging system (Li-COR Biotechnology).

### Histology, Immunohistochemistry analysis, and Masson's trichrome staining

Histological and immunohistochemical (IHC) analyses were performed as described previously (9). Briefly, formalin-fixed uterine and oviduct tissues were embedded in paraffin and sectioned to 5-μm thickness. The antibodies used were anti-ESR1 (13) (Thermo Fisher Scientific, Cat# MA5-13191) at a dilution of 1:200 ($n$ = 3 mice/genotype). Ki67 antibody (14) (BD Pharminogen, 550 609) was diluted at 1:100. TUNEL staining was performed using ApopTag Plus Peroxidase In Situ Apoptosis Kit (Millipore, #S7101) according to manufacturer's protocol ($n$ = 3–5 mice/genotype). Masson's trichrome staining was performed using a procedure previously described ($n$ = 3–5 mice/genotype) (15).

### Oocyte and embryo collection

$Esr1^{f/f}$ and $Pgr^{Cre}$*Esr1*KO females (4–6 weeks old) were superovulated with pregnant mare's serum gonadotropin (Calbiochem, Gibbstown, NJ, US) 5 IU intraperitoneally (i.p.) followed 48 h later by human chorionic gonadotropin (hCG; Calbiochem) 5 IU i.p. as described previously (16). The cumulus–oocyte complexes were collected from the oviduct at 18 h after hCG administration. The cumulus cells were washed

off with 0.1% hyarulonidase in phosphase buffered saline. The ovulated oocytes at metaphase II stage were counted and recorded ($n$ = 13 mice/genotype). For embryo collection, *Esr1*$^{f/f}$ and *Pgr*$^{Cre}$*Esr1*KO females (4–6 weeks old) were superovulated with pregnant mare's serum gonadotropin and hCG. Immediately after hCG injection, females were housed singly with a B6D2F1/J male (Jackson Laboratory, Bar Harbor, ME, US) overnight. Females with a copulatory plug the next morning were considered pregnant at 0.5 dpc. Zygotes (1-cell embryos) and 2-cell embryos were flushed from the oviduct at 11:00 AM on 0.5 dpc and 9:00 AM on 1.5 dpc ($n$ = 3–6 mice/genotype/time point). Morulae and blastocysts were collected from the oviduct and uterus at 3.5 dpc ($n$ = 3–6 mice/group/time point). Some of the tissues were collected at 4.5 dpc for histological analysis ($n$ = 3–4 mice/genotype).

### Measurement of serum $P_4$ and $E_2$ levels and quantification of corpus luteum number at 3.5 dpc

Blood samples and ovaries were collected from female mice at 3.5 dpc at ~11:00 AM. After $CO_2$ asphyxiation, blood samples were drawn from the inferior vena cava, then centrifuged at 7,000 g for 7 min. Sera were then frozen at –80°C and shipped to University of Virginia Center for Research in Reproduction Ligand Core for $P_4$ assay ($n$ = 3–9 mice/group). Serum estradiol ($E_2$) levels were determined using CalBiotech $E_2$ assay kit (#ES180S-100, CalBiotech, El Cajon, CA, US) as recommended by University of Virginia Center for Research in Reproduction Ligand Core (17). $E_2$ assay was performed in duplicate according to manufacturer's protocol using 25 µL serum from each animal ($n$ = 3–9 mice/group). Ovaries were fixed in 10% formalin and processed using standard histological procedures. Ovarian tissues were then sectioned and stained with H&E. Number of corpora lutea (CL)/section from both ovaries of each animal were counted and averaged ($n$ = 3–4 mice/genotype).

### RNA extraction and real-time polymerase chain reaction analysis

Ribonucleic acid (RNA) was extracted, and semiquantitative polymerase chain reaction and the analysis were carried out as previously described (18). Expression values were normalized to *Rpl7* expression and calculated as fold-change compared to vehicle-treated *Esr1*$^{f/f}$ uteri ($n$ = 3–6 mice/genotype) or *Esr1*$^{f/f}$ uteri at 3.5 dpc ($n$ = 5–8 mice/genotype). The primer sequences are listed in Table 1.

### Statistical analysis

Data were analyzed using GraphPad Prism version 5.00 for Mac OS X. All data were evaluated for statistically significant differences ($P < .05$) using 2-tailed unpaired Student's $t$-test or a 2-way analysis of variance with Sidak's multiple comparisons test.

## Results

### Lack of ESR1 expression in the oviduct and uterus leads to female infertility

To validate the specificity of *Esr1* deletion, IHC was performed in the uterine and oviductal tissues from ovarian intact 5- to 8-week-old female mice. In *Esr1*$^{f/f}$ control littermates, positive staining of ESR1 (13) was detected in every cell type in the oviduct (Fig. 1A) and the uterus (Fig. 1B). Consistent with the previous study, the recombinatory activity of *Pgr*$^{Cre}$ was observed in the isthmic but not the ampullary region of the oviduct (8), leading to a loss of ESR1 expression only in the isthmus in *Pgr*$^{Cre}$*Esr1*KO mice (Fig. 1A). In the uterus, ESR1 protein was not detected in the epithelial, stromal, or circular myometrial cells (Fig. 1B). Expression of ESR1 in some of the longitudinal myometrium remained intact in *Pgr*$^{Cre}$*Esr1*KO mice. We also found that there were no pups born to

**Table 1. List of primer sequences**

| Primers | Entrez gene name | Sequences: forward (F) and reverse (R): 5'→3' |
|---|---|---|
| *Birc1a* | Baculoviral inhibitor of apoptotic proteins repeat containing 1 | F: AGTGAGAAGGCAGCAAGCAG<br>R: CGCAGTCTCCTGGTTAGCAC |
| *Igfbp3* | Insulin-like growth factor binding protein 3 | F: GCAGGCAGCCTAAGCACCTA<br>R: TGCTCCTCCTCGGACTCACT |
| *Igfbp5* | Insulin-like growth factor binding protein 5 | F: TCTCCAGGCTCCCTCTTTCTC<br>R: TGATCACCATTTTCTCGGAGTCT |
| *Klf9* | Kruppel-like factor 9 | F: GGAAACACGCCTCCGAAA<br>R: GGGCTTTAAGATGGGAGGATTT |
| *Mad2l1* | MAD2 mitotic arrest deficient-like 1 | F: TGGTAGTGTTCTCCGTTCGATCT<br>R: GCAGGGTGATGCCTTGCT |
| *Nr4a1* | Nuclear receptor subfamily 4 group A member 1 | F: GGGCATGGTGAAGGAAGTTGT<br>R: GAGGCTGCTTGGGTTTTGAA |
| *Rpl7* | Ribosomal protein L7 | F: AGCTGGCCTTTGTCATCAGAA<br>R: GACGAAGGAGCTGCAGAACCT |
| *Txnip* | Thioredoxin-interacting protein | F: ACCACTTTCTCGGATGTTGGA<br>R: GGAAAGACAACGCCAGAAGGT |

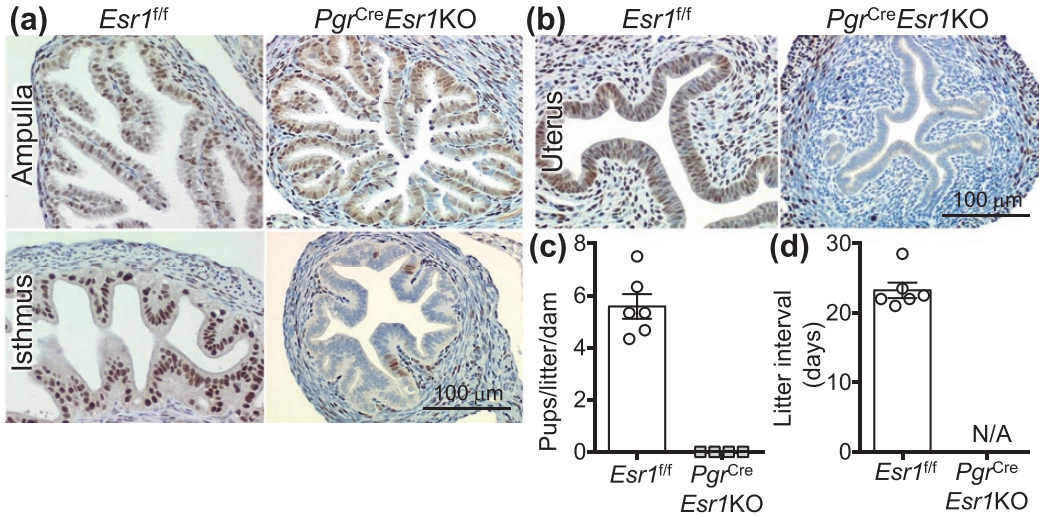


**Figure 1.** Loss of ESR1 expression in the isthmic region of the oviduct and the uterus leads to female infertility. Immunohistochemistry of ESR1 in (A) the ampullary and isthmic regions of the oviduct and (B) the uterus from *Esr1*$^{f/f}$ and *Pgr*$^{Cre}$*Esr1*KO female mice (at 5–8 weeks old). Representative images are shown ($n$ = 3 mice/genotype). Scale bars = 100 µm. (C) Number of pups/litter/dam and (D) the interval (days) between each litter in each dam after 6-month breeding trial with a fertile WT male ($n$ = 4–6 mice/genotype). Each data point represents one biological replicate. Abbreviation: N/A, not applicable as there were no pups born to *Pgr*$^{Cre}$*Esr1*KO females.

*Pgr*$^{Cre}$*Esr1*KO after a 6-month fertility trial compared to an average of 5.6 pups/litter/dam in *Esr1*$^{f/f}$ females (Figs. 1C and 1D). Therefore, a loss of ESR1 in the isthmus of the oviduct and the uterus may contribute to infertility of *Pgr*$^{Cre}$*Esr1*KO mice.

## Blunted ESR1 expression in the pituitary gland is associated with aberrant ovarian function

Due to the expression of *Pgr*$^{Cre}$ in the pituitary gland (6), it was possible that the hypothalamus–pituitary–gonadal (HPG) axis was altered in *Pgr*$^{Cre}$*Esr1*KO mice. Therefore, we evaluated the expression of ESR1 protein in *Pgr*$^{Cre}$*Esr1*KO compared to *Esr1*$^{f/f}$ females. Consistent with prior observations (19), we found that *Pgr*$^{Cre}$*Esr1*KO had lower expression level of ESR1 (11) in pituitary glands compared to *Esr1*$^{f/f}$ females (Fig. 2A), suggesting a partial deletion of *Esr1* in some but not all cell types in the pituitary gland. Circulating LH was significantly higher in *Pgr*$^{Cre}$*Esr1*KO than in *Esr1*$^{f/f}$ females (Fig. 2B). Additionally, vaginal cytological analysis showed a persistent diestrus stage in *Pgr*$^{Cre}$*Esr1*KO compared to *Esr1*$^{f/f}$ females (Fig. 2C). *Pgr*$^{Cre}$*Esr1*KO females also exhibited hemorrhagic cysts with no apparent CL when collected at 12 weeks old compared to *Esr1*$^{f/f}$ ovaries (Fig. 2D). These findings suggest that disruption of the HPG axis in *Pgr*$^{Cre}$*Esr1*KO mice could also contribute to the female fertility defect. However, when stimulated with exogenous gonadotropins during the postpubertal period (5–8 weeks old), before hemorrhagic cysts developed, *Pgr*$^{Cre}$*Esr1*KO females showed a comparable number of ovulated oocytes compared to *Esr1*$^{f/f}$ females (Fig. 2E).

## Defective embryo transport in Pgr$^{Cre}$Esr1KO female mice

Our previous findings showed that conditional knockout of *Esr1* in all epithelial cells throughout the female reproductive tract disrupts preimplantation embryo development and proper movement of embryos from the oviduct to the uterus (16, 20). To investigate the effect of ESR1 loss in the isthmus region alone on preimplantation embryo development and transport, embryos were collected from the oviduct and uterus at 0.5, 1.5, and 3.5 dpc for 1-cell embryos (zygotes), 2-cell embryos, and morulae/blastocysts, respectively. In this study, 5- to 8-week-old females were used to avoid potential confounding effects of hemorrhagic cysts observed at 12 weeks.

Comparable percentages of 1-cell and 2-cell embryos were retrieved from *Esr1*$^{f/f}$ and *Pgr*$^{Cre}$*Esr1*KO oviducts at 0.5 and 1.5 dpc, respectively (Fig. 3A). At 3.5 dpc, there was no significant difference in percentages of blastocyst and morulae retrieved from *Esr1*$^{f/f}$ and *Pgr*$^{Cre}$*Esr1*KO oviducts and uteri (Fig. 3C). However, it was noted that the percentage of nonviable embryos appeared to be slightly higher in *Pgr*$^{Cre}$*Esr1*KO females but not significantly different from *Esr1*$^{f/f}$ mice (Fig. 3C). More important, all embryos were retrieved only from the oviducts of *Pgr*$^{Cre}$*Esr1*KO females, whereas all embryos were located in the uterus of *Esr1*$^{f/f}$ females at 3.5 dpc (Figs. 4A and 4B). Using histological analysis, we found that embryos (blastocysts) were retained in the ampullary region of *Pgr*$^{Cre}$*Esr1*KO mice at 3.5 dpc whereas embryos in *Esr1*$^{f/f}$ were located in the uterus (Fig. 4C). There were no embryos found in

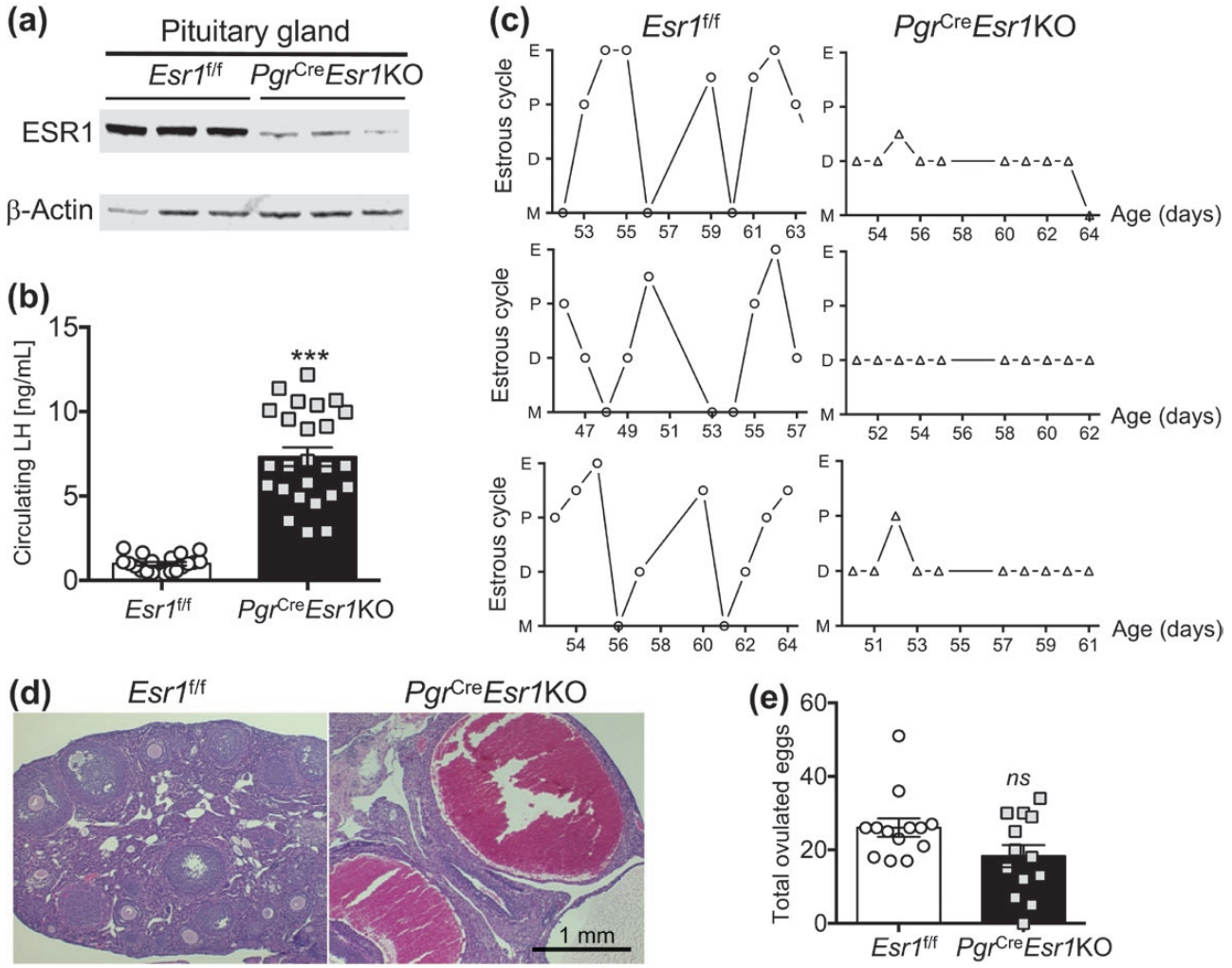


**Figure 2.** Deletion of ESR1 in the pituitary gland altered the HPG-axis. (A) ESR1 expression in pituitary glands from *Pgr*$^{Cre}$*Esr1*KO compared to *Esr1*$^{f/f}$ adult females ($n$ = 3 mice/genotype). β-actin was used as a loading control for each sample. (B) Serum LH levels from ovary-intact females at 8 to 9 weeks of age in randomly cycling females ($n$ = 20–25 mice/genotype). ***$P$ < .001, significantly different from *Esr1*$^{f/f}$; unpaired 2-tailed Student's $t$-test. (C) Vaginal smear in *Pgr*$^{Cre}$*Esr1*KO compared to *Esr1*$^{f/f}$ females at the age of 47 to 64 days old ($n$ = 7–10 mice/genotype). Three representative animals shown for each group. (D) H&E staining of cross-sections of ovaries from adult *Esr1*$^{f/f}$ and *Pgr*$^{Cre}$*Esr1*KO females. Representative images are shown ($n$ = 4 mice/genotype). Scale bar = 1 mm. (e) Number of total oocytes ovulated in the oviduct after gonadotropin treatment at 5 to 7 weeks of age ($n$ = 13 mice/genotype). Each data point represents one biological replicate. Abbreviations: E, estrus; D, diestrus; M, metestrus; *ns;* not significantly different from *Esr1*$^{f/f}$ females; P, proestrus.

the uterine lumen of *Pgr*$^{Cre}$*Esr1*KO females at 3.5 dpc (Fig. 4C). At 4.5 dpc, all embryos were attached to the uterine wall of *Esr1*$^{f/f}$ controls while the embryos were restricted to the isthmic region of *Pgr*$^{Cre}$*Esr1*KO mice (Fig. 4D).

It is well established that disruption of circulating $P_4$ levels leads to embryo transport arrest in the oviduct (21). To determine whether the embryo transport defect in *Pgr*$^{Cre}$*Esr1*KO females was due to $P_4$ deficiency, we investigated whether CL (source of $P_4$ production) were present in the ovaries. At 3.5 dpc, the number of CL in *Pgr*$^{Cre}$*Esr1*KO was not significantly different from *Esr1*$^{f/f}$ ovaries ($P$ = .8366) (Figs. 4E and 4F). However, serum $P_4$ levels were significantly less in *Pgr*$^{Cre}$*Esr1*KO compared to *Esr1*$^{f/f}$ females (Fig. 4G), while serum $E_2$ levels were not significantly different but trended toward an elevation ($P$ = .0636) (Fig. 4H). These results indicate that female mice lacking ESR1 in the isthmic region of the oviduct and the uterus exhibit impaired embryo transport and that this transport defect could be due to a reduced circulating $P_4$, a lack of proper estrogen signaling in the oviduct epithelial cells, or both.

### Loss of ESR1 leads to increased apoptosis and blunted estrogen-induced uterine transcripts

Because we observed an increased number of cells with apoptotic-like bodies in the *Pgr*$^{Cre}$*Esr1*KO uteri at 3.5 dpc (Fig. 4C), we evaluated the presence of an apoptotic cell marker (TUNEL staining). Positive TUNEL staining was detected in *Pgr*$^{Cre}$*Esr1*KO uteri at

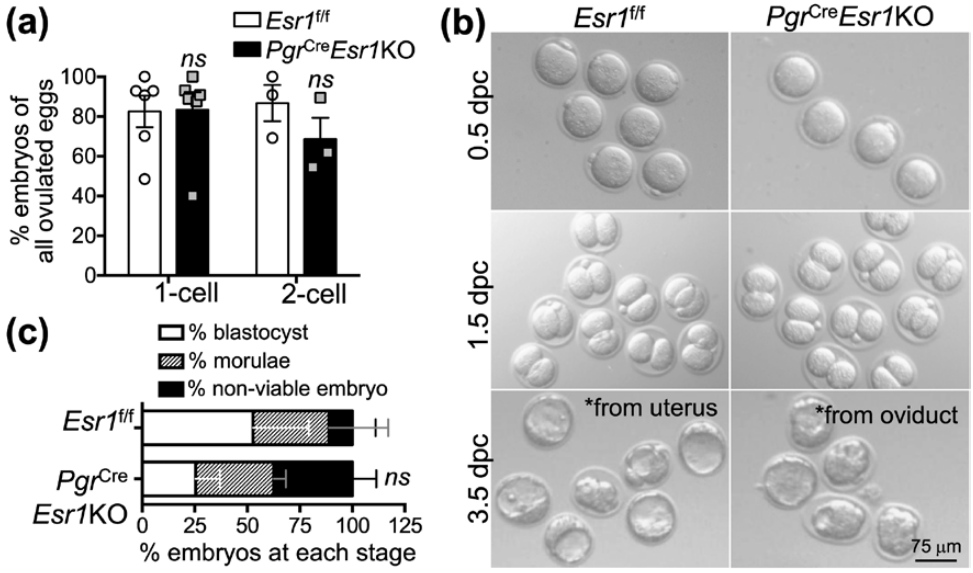


**Figure 3.** Loss of ESR1 in the isthmic region of the oviduct and the uterus leads to defective embryo transport. (A) Percentage of embryos at 1-cell or 2-cell stages of total ovulated eggs in *Esr1*$^{f/f}$ and *Pgr*$^{Cre}$*Esr1*KO females ($n$ = 3–6 mice/genotype/time point). Each data point represents one biological replicate. (B) Representative images of 1-cell, 2-cell embryos, and morulae/blastocysts collected at 0.5, 1.5, and 3.5 dpc, respectively from *Esr1*$^{f/f}$ and *Pgr*$^{Cre}$*Esr1*KO oviducts and uteri ($n$ = 3–6 mice/group/time point). Scale bar = 75 µm. (C) Percentage of blastocysts, morulae, or nonviable embryos collected from *Esr1*$^{f/f}$ and *Pgr*$^{Cre}$*Esr1*KO oviducts and uteri at 3.5 dpc. Abbreviation: *ns;* not significantly different from *Esr1*$^{f/f}$ females. *At 3.5 dpc, all embryos collected from *Pgr*$^{Cre}$*Esr1*KO were from the oviduct, not the uterus.

3.5 dpc; however, staining was not detected in *Esr1*$^{f/f}$ controls (Fig. 5A). Our previous findings indicated that a loss of ESR1 in uterine epithelial cells correlates with a decrease in an inhibitor of apoptotic proteins called baculoviral inhibitors of apoptosis repeat-containing 1 (or *Birc1a*), an estrogen-target gene (9). In this study, we found a blunted *Birc1a* expression in *Pgr*$^{Cre}$*Esr1*KO compared to *Esr1*$^{f/f}$ uteri (Fig. 5B). Moreover, there was more connective and fibrotic tissue detected in *Pgr*$^{Cre}$*Esr1*KO at 3.5 dpc compared to *Esr1*$^{f/f}$ uteri as indicated by the blue coloration in Masson's trichrome histological analysis (Fig. 5C).

To assess uterine responsiveness to estrogen in the ovariectomized uteri, uterine wet weight was measured 24 h after treatment with $E_2$ at a dose of 0.25 µg/mouse. Uterine weight increased significantly in *Esr1*$^{f/f}$ controls (Fig. 6A); however, there was no change in uterine weight after $E_2$ treatment in *Pgr*$^{Cre}$*Esr1*KO uteri. In agreement with the uterine weight gain, $E_2$ stimulated DNA synthesis (EdU incorporation) (Fig. 6B) and cell proliferation (Ki67 IHC) (14) (Fig. 6C) only in *Esr1*$^{f/f}$, not *Pgr*$^{Cre}$*Esr1*KO uteri. Estrogen-target genes (5, 10, 18) such as MAD2 mitotic arrest deficient-like 1 (*Mad2l1*), Kruppel-like factor 9 (*Klf9*), nuclear receptor subfamily 4 group A member 1 (*Nr4a1*), and insulin-like growth factor binding protein 5 (*Igfbp5*) were increased in $E_2$-treated *Esr1*$^{f/f}$ uteri. However, the expression of these estrogen-target genes was not stimulated by $E_2$ in *Pgr*$^{Cre}$*Esr1*KO uteri. Known estrogen downregulated genes (10, 22) such as insulin-like growth factor binding protein 3 (*Igfbp3*) and thioredoxin-interacting protein (*Txnip*) were significantly reduced in $E_2$-treated *Pgr*$^{Cre}$*Esr1*KO but at a lesser extent compared to $E_2$-treated *Esr1*$^{f/f}$ uteri. These data suggest that expression of ESR1 in the uterus is required for $E_2$-regulation of gene expression as well as modulation of uterine apoptosis.

## Discussion

The reproductive phenotype—female infertility—found in *Pgr*$^{Cre}$*Esr1*KO female mice recapitulates findings from the previous αERKO mouse models (1, 5). However, the information gained from the present study is that ESR1 expression specifically within the oviductal isthmus is required for normal embryo transport out of the oviduct, which has not been previously reported. Our recent study shows that deletion of *Esr1* in the epithelial cells of the entire length of the female reproductive tract using *Wnt7a*$^{Cre/+}$/*Esr1*$^{f/f}$ mice causes both embryo death prior to the 2-cell stage and an embryo transport defect (16, 20). Since *Pgr*$^{Cre}$*Esr1*KO mice showed a deletion of *Esr1* only in the isthmic region and did not have significant changes in embryo development, it indicates that the embryo death phenotype observed in *Wnt7a*$^{Cre/+}$/*Esr1*$^{f/f}$ females was specific to the loss of ESR1 in the ampullary region. As such, embryo transport through the oviduct was regulated by the action of ESR1 in the isthmic region (summarized in Fig. 7). Importantly, it is likely that the embryo transport defect in *Pgr*$^{Cre}$*Esr1*KO could also

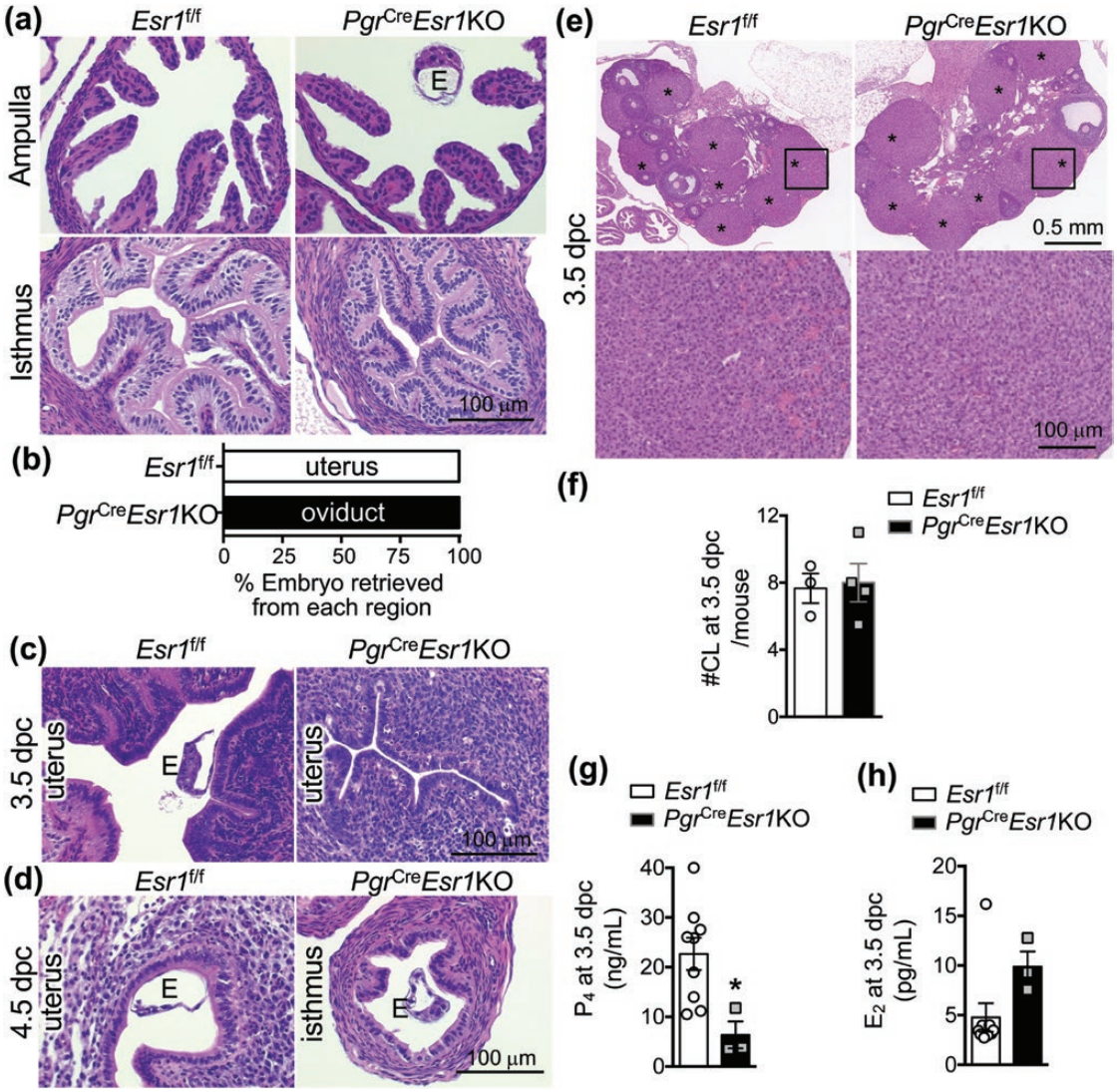


**Figure 4.** Embryo retention in the oviduct at 3.5 and 4.5 dpc in the absence of ESR1 in the isthmic region of the oviduct and the uterus. (A) Histological analysis using H&E staining of the ampullary and isthmic region of the oviduct from *Esr1*$^{f/f}$ and *Pgr*$^{Cre}$*Esr1*KO female mice at 3.5 dpc ($n$ = 3–4 mice/genotype). Representative images are shown. (B) Percentage of embryos collected at 3.5 dpc from the uterus or the oviduct ($n$ = 3–5 mice/genotype). (C) Uterine histology at 3.5 dpc ($n$ = 3–4 mice/genotype). Representative images are shown. (D) The location of the embryo in the uterus or the oviduct at 4.5 dpc ($n$ = 3–4 mice/genotype). Scale bars = 100 µm. (E) H&E staining of ovarian sections collected at 3.5 dpc ($n$ = 3–4 mice/genotype). Lower panels are higher magnification to illustrate luteal cells. Boxes show areas used for higher magnification images. Scale bars = 0.5 mm in the upper panel and 100 µm in the lower panel. (F) Average numbers of CL/field image/mouse at 3.5 dpc ($n$ = 3–4 mice/genotype). (G) Serum $P_4$ (ng/mL) and (H) $E_2$ (pg/mL) levels at 3.5 dpc ($n$ = 3–9 mice/genotype). *$P < 0.05$; significantly different from *Esr1*$^{f/f}$ controls. Abbreviation: E, embryo. *Corpus luteum.

result from reduced circulating $P_4$ levels (21). However, the mechanistic details of estrogen/ESR1 mediated control of embryo transport through the isthmus as well as a confounding factor from disrupted $P_4$ levels remain to be investigated. Future studies will address (i) whether a lack of appropriate $P_4$ levels is the sole source of the embryo transport defect in *Pgr*$^{Cre}$*Esr1*KO females, (ii) the cause of $P_4$ deficiency in *Pgr*$^{Cre}$*Esr1*KO mice, and (iii) whether the development of pre-implantation embryos at 1.5, 2.5, and 3.5 dpc is affected by the reduction of circulating $P_4$.

In mammals, the epithelial layer of the isthmus consists mostly of secretory cells with fewer ciliated cells compared to the ampullary region (23–25). It is postulated that embryo transport in the oviduct is controlled by two major physiological responses: (i) ciliary activity and (ii) muscle contractility (26, 27). These responses are responsible for generating oviductal fluid flow through ciliary beating and muscle contractions but also play a role in sperm migration and fertilization (28, 29). Our previous observation was that a loss of ESR1 in the epithelial cells of the entire length of the oviduct caused an overall decrease in ciliary beat frequency (20). In the present study, the deletion of *Esr1* was restricted to the isthmic region and not the ampulla where the ciliated

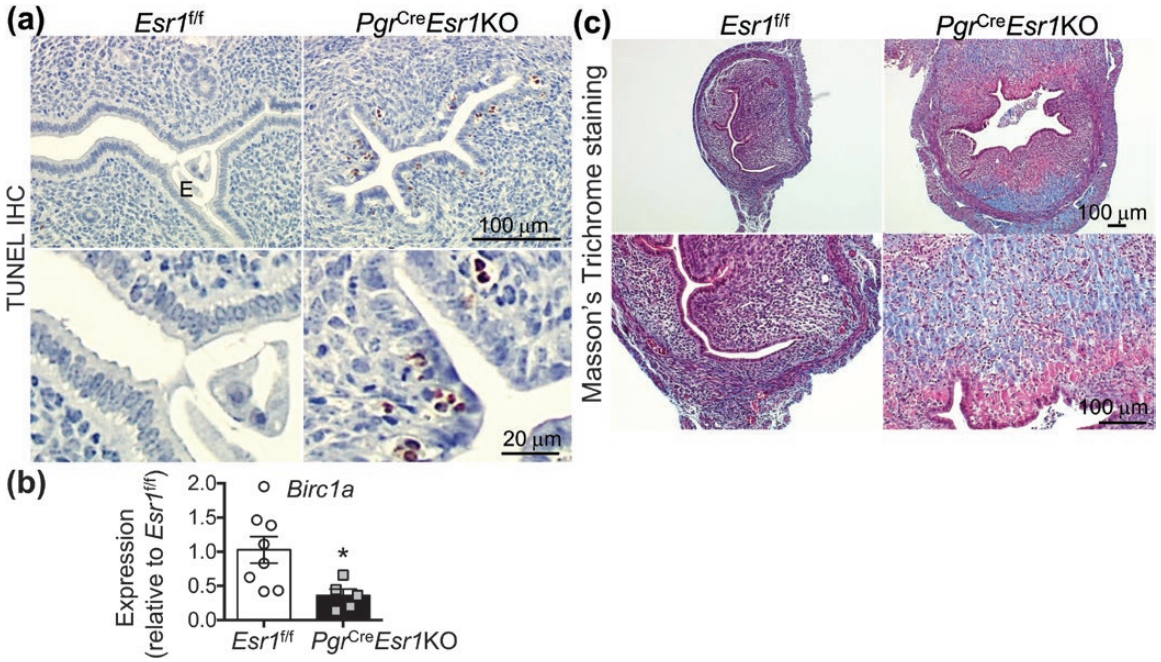


**Figure 5.** Deletion of ESR1 from uterine tissue causes increased apoptosis and uterine collagenous content. (A) Immunohistochemistry of TUNEL at 3.5 dpc in *Esr1*$^{f/f}$ and *Pgr*$^{Cre}$*Esr1*KO uteri ($n$ = 3–5 mice/genotype). Representative images are shown. Scale bars = 100 μm and 20 μm for top and bottom panels, respectively. (B) *Birc1a* transcript in *Esr1*$^{f/f}$ and *Pgr*$^{Cre}$*Esr1*KO uteri at 3.5 dpc ($n$ = 5–8 mice/genotype). Each data point represents one biological replicate. *$P$ < .05, significantly different from *Esr1*$^{f/f}$; unpaired 2-tailed Student's $t$-test. (c) Masson's trichrome staining of *Esr1*$^{f/f}$ and *Pgr*$^{Cre}$*Esr1*KO uteri at 3.5 dpc. Blue staining indicates collagen and connective tissues. Pink and red staining indicate keratin and muscle fibers ($n$ = 3–5 mice/genotype). Scale bars = 100 μm. Representative images are shown.

epithelial cells are abundant. Therefore, the expression of ESR1 remains intact in the ciliated epithelial cells of the ampullary region. Thus, it seems unlikely that impaired embryo transport observed in *Pgr*$^{Cre}$*Esr1*KO female mice results from changes in ciliary function.

The action of steroid hormones on oviduct contractility appears to be species-specific. In rabbits, estrogen treatment decreases the contractility of the oviduct (30). In cows, estrogen treatment increases the levels of prostaglandin and endothelin, which could, in turn, stimulate the contraction of the oviductal muscle layer (31–33). It is possible that estrogen directly modulates oviductal muscle contraction through production of prostaglandins and endothelins (31–33). However, direct mechanistic action of ESR1 regulation of oviductal muscle contraction remains unclear. Nevertheless, the reduced contractile function of the muscle cells could lead to a retention of embryos inside the oviduct. This phenomenon is called tube-locking (34) due to an exogenous pharmacological estrogen, which was observed in several species including guinea pig, hamster, mouse, and rabbit (34). These findings indicate that the action of estrogen through ESR1 in the oviduct has to be fine-tuned to precisely govern embryo transport from the oviduct to the uterine lumen via the regulation of muscle contraction in the isthmic region. $P_4$, through PGR, induces muscle contraction in the oviduct of the rabbit (30). Microarray data from oviductal tissues of *Pgr* knockout mice showed that levels of several genes with functional annotation of muscle contractility were aberrantly expressed in the oviduct of *Pgr* knockout mice (35). Since estrogen controls the expression of PGR in the female reproductive tract (36), it is also possible that estrogen modulates its oviductal contractility through the regulation of $P_4$/PGR-mediated signaling.

In addition to effects on oviductal function, we also found that partial deletion of *Esr1* in the pituitary gland disrupted the HPG axis and induced an elevation of LH levels, which is in agreement with findings from previous studies (19). Laws et al demonstrated that, in addition to elevated LH levels, serum $P_4$ as well as $E_2$ and testosterone at 6 months old were significantly higher in *Pgr*$^{Cre}$*Esr1*KO compared to control littermates (19). Elevated levels of steroids are likely due to a lack of estrogen-mediated negative feedback in the pituitary causing an overstimulation of ovarian cells by LH resulting in an increased steroidogenesis. Our laboratory also reported that the formation of hemorrhagic ovarian cysts is due to a high circulatory level of LH (37). However, we found that *Pgr*$^{Cre}$*Esr1*KO female mice could be stimulated with exogenous gonadotropins to induce ovulation at levels comparable to control littermates at 5 to 8 weeks of age, prior to the presence of hemorrhagic cysts, whereas the previous αERKO mouse model showed defective ovulation (38). In agreement with this, CL numbers at 3.5 dpc in *Pgr*$^{Cre}$*Esr1*KO were equivalent to that of controls

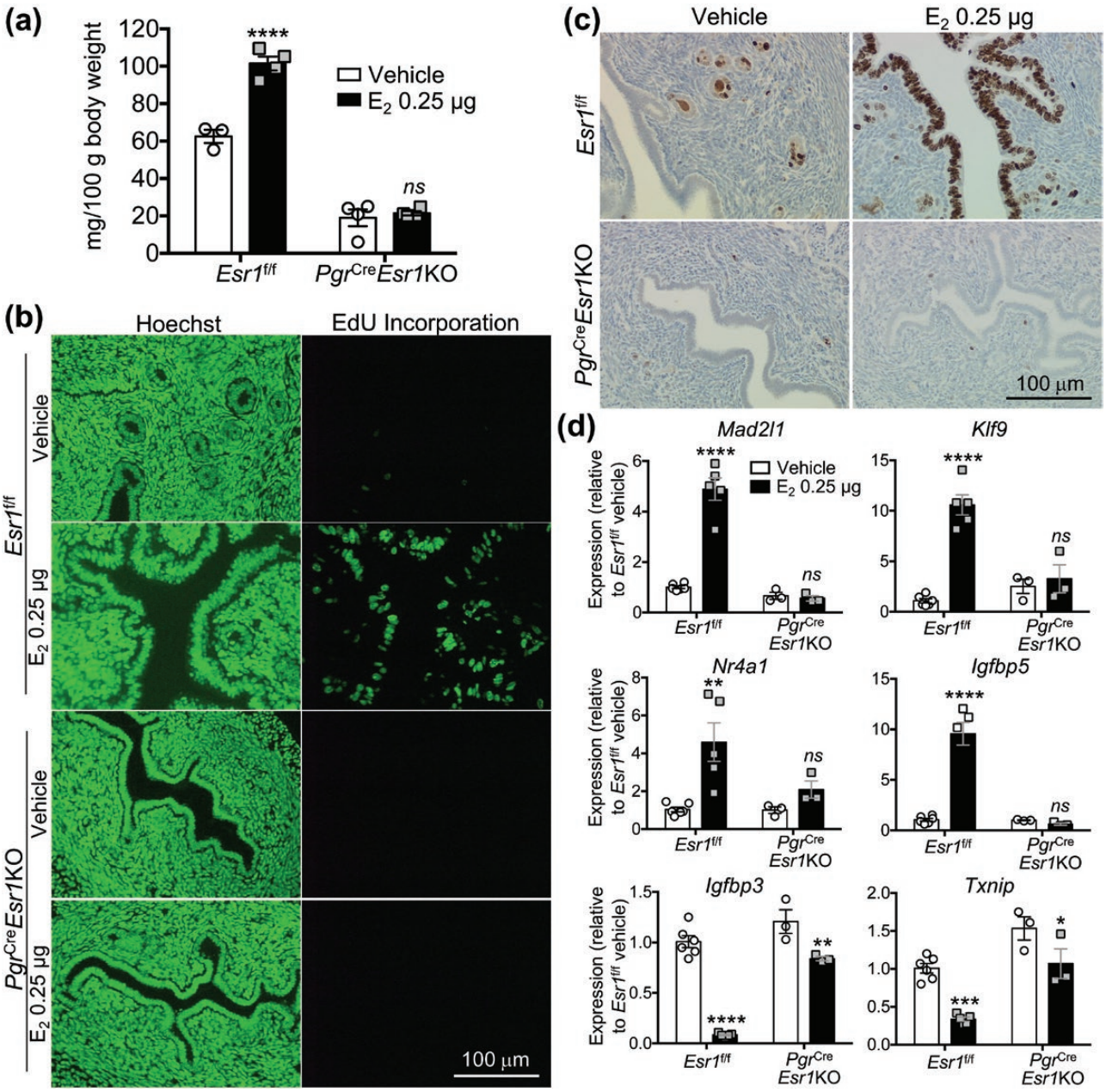


**Figure 6.** Loss of $E_2$-induced uterotrophic response in adult ovariectomized females lacking ESR1 expression. (A) Uterine weight (mg/100 g body weight), (B) newly synthesized DNA indicated by EdU incorporation, and (C) cell proliferation indicated by Ki67 immunohistochemistry in ovariectomized females treated with vehicle (100 µL sesame oil) or $E_2$ (0.25 µg/mouse) for 24 h prior to collection ($n$ = 3–4 mice/genotype/treatment). **** $P < .0001$, significantly different from vehicle within the same genotype; unpaired 2-tailed Student's $t$-test. *ns*; not significantly different from vehicle within the same genotype group. Hoechst indicates DNA staining. (D) Gene expression (*Mad2l1*, *Klf9*, *Nr4a1*, *Igfbp5*, *Igfbp3*, and *Txnip*) in *Esr1*$^{f/f}$ and *Pgr*$^{Cre}$*Esr1*KO uteri 24 h after treatment with Vehicle, or $E_2$ ($n$ = 3–6 mice/genotype/treatment). *, **, ***, and ****$P < .05$, 0.01, 0.001, and 0.0001, significantly different from vehicle treatment within the same genotype group. *ns*; not significantly different from vehicle within the same genotype group. Each data point represents one biological replicate.

when experiments were performed at 5 to 8 weeks old, suggesting that the development of CL was not affected at this age. However, a significant reduction of $P_4$ levels in *Pgr*$^{Cre}$*Esr1*KO indicates that CL function was disrupted. It is expected that CL development should not be disrupted in *Pgr*$^{Cre}$*Esr1*KO females, as ESR1 is expressed exclusively in the theca cells of the ovary (39) while Cre-recombinase activity driven by *Pgr* promoter should be active in the preovulatory granulosa and the luteal cells (6). Therefore, the presence of Cre and LoxP does not overlap; as such, folliculogenesis and granulosa cell differentiation to luteal cells should not be affected. Circulatory levels of $E_2$ at 3.5 dpc were not significantly different in *Pgr*$^{Cre}$*Esr1*KO compared to that of controls but trended toward an elevation. This is likely due to the fact that the $E_2$ level in one of the control animals was at 16 pg/mL. Therefore, it is possible that serum $E_2$ levels will be significantly higher if the number of animals in

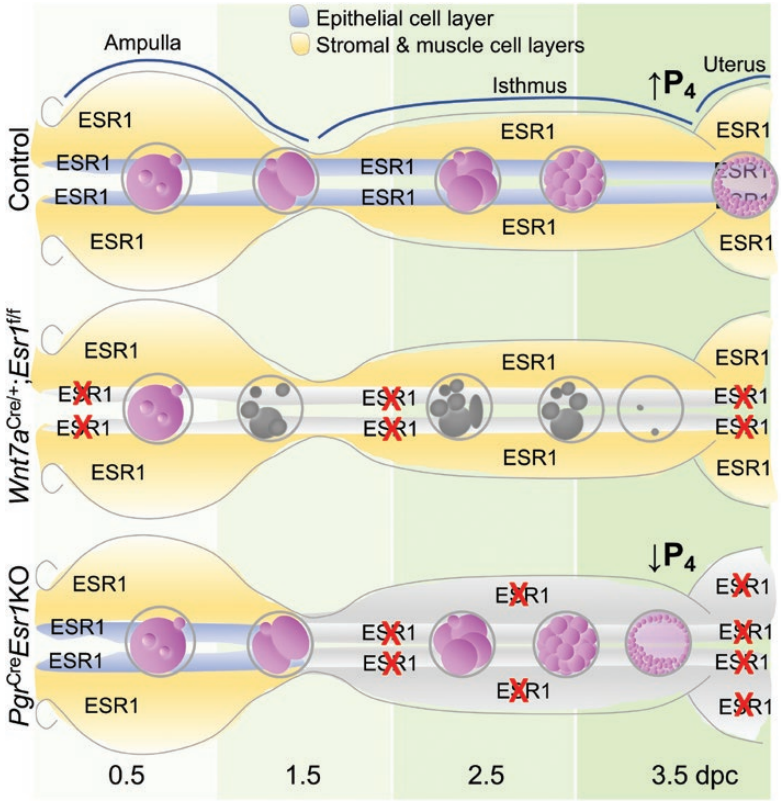


**Figure 7.** A summary of the effect of a loss of ESR1 in the epithelial cells (*Wnt7a*$^{Cre/+}$/*Esr1*$^{f/f}$) (16) or in the isthmic region of the oviduct (*Pgr*$^{Cre}$*Esr1*KO) on embryo development and transport in comparison to control animals. $P_4$ deficiency (↓$P_4$) was observed in *Pgr*$^{Cre}$*Esr1*KO mice compared to an elevated circulating level of $P_4$ (↑$P_4$) in control animals at 3.5 dpc. This finding suggests that expression of ESR1 in the isthmus and normal $P_4$ levels allow for successful embryo transport from the oviduct to the uterus. Gray embryos = nonviable embryos. The oviductal phenotype from the global deletion of *Esr1* was not depicted in the diagram as the mice are unable to mate or ovulate and the oviductal function of ESR1 was not evaluated. Abbreviations: dpc, days post coitus; ESR1, estrogen receptor α.

Antibody Table 1

| Peptide/Protein Target | Name of Antibody | Manufacturer, Catalog No., and/or Name of Individual Providing the Antibody | Species Raised in; Monoclonal or Polyclonal | Dilution Used | RRID |
|---|---|---|---|---|---|
| ESR1 (for IHC analysis) | Estrogen Receptor alpha (1D5) | Thermo Fisher Scientific Cat# MA5-13 191 | Mouse; monoclonal | 1:200 | AB_10986080 |
| ESR1 (for Western blotting) | ER alpha (MC-20) | Santa Cruz Biotechnology Cat# sc-542 | Rabbit, monoclonal | 1:650 | AB_631470 |
| Ki67 | Purified mouse anti-Ki67 | BD Pharminogen Cat #550 609 | Mouse; monoclonal | 1:100 | AB_393778 |
| β-Actin | Anti-beta-Actin | Sigma-Aldrich Cat# A2228 | Mouse; monoclonal | 1:2000 | AB_476697 |

*Pgr*$^{Cre}$*Esr1*KO group increased, which would be due to a defective feedback regulation of $E_2$ levels due to a disruption of the previously described HPG axis instead of a local defect for $E_2$ production in the *Pgr*$^{Cre}$*Esr1*KO ovaries.

In conclusion, our main observations resulting from studies using the *Pgr*$^{Cre}$*Esr1*KO mouse model highlight the necessity of estrogen signaling through ESR1 in oviduct function during embryo transport, likely via a direct regulation of estrogen signal or indirectly through $P_4$/PGR action in the isthmic region. In humans, ectopic or tubal pregnancy, caused by embryo retention and attachment within the Fallopian tubes, is one of the leading causes of maternal death due to severe internal bleeding (40). Although tubal ectopic pregnancy would appear to be restricted to primates (41), our studies support clinical findings that the expression of ESR1 was decreased or absent in the Fallopian tubes from patients with ectopic pregnancy (42, 43). Accordingly, our findings have the potential to provide a better understanding for the etiology of ectopic pregnancy and specifically, why the embryo is retained and implants in the Fallopian tube instead of the uterine wall.

## Acknowledgements

We thank the NIEHS Histology and Immunohistology Core for tissue processing and TUNEL and Masson's Trichrome staining, NIEHS Comparative Medicine Branch for surgery and animal care, and Drs. Miranda Bernhardt and Rong Li for critical suggestions for this manuscript.

***Financial Support:*** Financial support to KFR was provided through Dr. Humphrey Yao at the NIEHS. This study is supported by NIH/NIEHS 1ZIAES102965 to KJR, 1ZIAES103311 to FJD, 1ZIAES102405 to CJW, 1ZIAES070065 to KSK, the Eunice Kennedy Shriver NIH/NICHD to R01HD042311 JPL, and R01HD097087 to WW.

## Additional Information

***Correspondence:*** Wipawee Winuthayanon, Biotechnology/Life Science Building, 1770 Stadium Way, Pullman, WA, US 99164. E-mail: w.winuthayanon@wsu.edu.

***Disclosure Summary:*** The authors have nothing to disclose.

## References

1. Lubahn DB, Moyer JS, Golding TS, Couse JF, Korach KS, Smithies O. Alteration of reproductive function but not prenatal sexual development after insertional disruption of the mouse estrogen receptor gene. *Proc Natl Acad Sci U S A*. 1993;**90**(23):11162–11166.
2. Smith EP, Boyd J, Frank GR, et al. Estrogen resistance caused by a mutation in the estrogen-receptor gene in a man. *N Engl J Med*. 1994;**331**(16):1056–1061.
3. Quaynor SD, Stradtman EW Jr, Kim HG, et al. Delayed puberty and estrogen resistance in a woman with estrogen receptor α variant. *N Engl J Med*. 2013;**369**(2):164–171.
4. Krege JH, Hodgin JB, Couse JF, et al. Generation and reproductive phenotypes of mice lacking estrogen receptor beta. *Proc Natl Acad Sci U S A*. 1998;**95**(26):15677–15682.
5. Hewitt SC, Kissling GE, Fieselman KE, Jayes FL, Gerrish KE, Korach KS. Biological and biochemical consequences of global deletion of exon 3 from the ER alpha gene. *FASEB J*. 2010;**24**(12):4660–4667.
6. Soyal SM, Mukherjee A, Lee KY, et al. Cre-mediated recombination in cell lineages that express the progesterone receptor. *Genesis*. 2005;**41**(2):58–66.
7. Cui T, He B, Kong S, et al. PR-Set7 deficiency limits uterine epithelial population growth hampering postnatal gland formation in mice. *Cell Death Differ*. 2017;**24**(12):2013–2021.
8. Daikoku T, Yoshie M, Xie H, et al. Conditional deletion of Tsc1 in the female reproductive tract impedes normal oviductal and uterine function by enhancing mTORC1 signaling in mice. *Mol Hum Reprod*. 2013;**19**(7):463–472.
9. Winuthayanon W, Hewitt SC, Orvis GD, Behringer RR, Korach KS. Uterine epithelial estrogen receptor α is dispensable for proliferation but essential for complete biological and biochemical responses. *Proc Natl Acad Sci U S A*. 2010;**107**(45):19272–19277.
10. Hewitt SC, Deroo BJ, Hansen K, et al. Estrogen receptor-dependent genomic responses in the uterus mirror the biphasic physiological response to estrogen. *Mol Endocrinol*. 2003;**17**(10):2070–2083.
11. RRID:AB_631470. http://antibodyregistry.org/search?q=AB_631470.
12. RRID:AB_476697. http://antibodyregistry.org/search?q=AB_476697.
13. RRID:AB_10986080. http://antibodyregistry.org/search.php?q=AB_10986080.
14. RRID:AB_393778. http://antibodyregistry.org/search?q=AB_393778.
15. Li S, Herrera GG, Tam KK, Lizarraga JS, Beedle MT, Winuthayanon W. Estrogen action in the epithelial cells of the mouse vagina regulates neutrophil infiltration and vaginal tissue integrity. *Sci Rep*. 2018;**8**(1):11247.
16. Winuthayanon W, Bernhardt ML, Padilla-Banks E, et al. Oviductal estrogen receptor α signaling prevents protease-mediated embryo death. *Elife*. 2015;**4**:e10453.
17. Haisenleder DJ, Schoenfelder AH, Marcinko ES, Geddis LM, Marshall JC. Estimation of estradiol in mouse serum samples: evaluation of commercial estradiol immunoassays. *Endocrinology*. 2011;**152**(11):4443–4447.
18. Winuthayanon W, Hewitt SC, Korach KS. Uterine epithelial cell estrogen receptor alpha-dependent and -independent genomic profiles that underlie estrogen responses in mice. *Biol Reprod*. 2014;**91**(5):110.
19. Laws MJ, Kannan A, Pawar S, Haschek WM, Bagchi MK, Bagchi IC. Dysregulated estrogen receptor signaling in the hypothalamic-pituitary-ovarian axis leads to ovarian epithelial tumorigenesis in mice. *Plos Genet*. 2014;**10**(3):e1004230.
20. Li S, O'Neill SR, Zhang Y, et al. Estrogen receptor α is required for oviductal transport of embryos. *FASEB J*. 2017;**31**(4):1595–1607.
21. Kendle KE, Lee B. Investigation of the influence of progesterone on mouse embryo transport by using antiprogestational steroids. *J Reprod Fertil*. 1980;**58**(1):253–258.
22. Deroo BJ, Hewitt SC, Peddada SD, Korach KS. Estradiol regulates the thioredoxin antioxidant system in the mouse uterus. *Endocrinology*. 2004;**145**(12):5485–5492.
23. Pauerstein CJ, Eddy CA. Morphology of the Fallopian tube. In: Keller FK, Schumacher GFB, eds. *The Biology of the Fluids of the Female Genital Tract*. Amsterdam, The Netherlands: Elsevier/North-Holland; 1979:299–317.
24. Stewart CA, Behringer RR. Mouse oviduct development. *Results Probl Cell Differ*. 2012;**55**:247–262.
25. Brenner RM, Maslar IA. The primate oviduct and endometrium. In: Knobil E, Neill JD, eds. *The Physiology of Reproduction*. 1st ed. New York, NY: Raven; 1988:303–327.
26. Lyons RA, Saridogan E, Djahanbakhch O. The reproductive significance of human Fallopian tube cilia. *Hum Reprod Update*. 2006;**12**(4):363–372.
27. Croxatto HB, Ortiz ME, Díaz S, Hess R, Balmaceda J, Croxatto HD. Studies on the duration of egg transport by the human oviduct. II. Ovum location at various intervals following luteinizing hormone peak. *Am J Obstet Gynecol*. 1978;**132**(6):629–634.
28. Hino T, Yanagimachi R. Active peristaltic movements and fluid production of the mouse oviduct: their roles in fluid and sperm transport and fertilizationdagger. *Biol Reprod*. 2019;**101**(1):40–49.
29. Miki K, Clapham DE. Rheotaxis guides mammalian sperm. *Curr Biol*. 2013;**23**(6):443–452.
30. Nozaki M, Ito Y. Changes in physiological properties of rabbit oviduct by ovarian steroids. *Am J Physiol*. 1987;**252**(6 Pt 2):R1059–R1065.
31. Wijayagunawardane MP, Miyamoto A, Taquahashi Y, et al. In vitro regulation of local secretion and contraction of the bovine oviduct: stimulation by luteinizing hormone, endothelin-1 and prostaglandins, and inhibition by oxytocin. *J Endocrinol*. 2001;**168**(1):117–130.
32. Wijayagunawardane MP, Miyamoto A, Sato K. Prostaglandin E2, prostaglandin F2 alpha and endothelin-1 production by cow oviductal epithelial cell monolayers: effect of progesterone, estradiol 17 beta, oxytocin and luteinizing hormone. *Theriogenology*. 1999;**52**(5):791–801.
33. Wijayagunawardane MP, Choi YH, Miyamoto A, et al. Effect of ovarian steroids and oxytocin on the production of

prostaglandin E2, prostaglandin F2alpha and endothelin-1 from cow oviductal epithelial cell monolayers in vitro. *Anim Reprod Sci*. 1999;**56**(1):11–17.
34. Greenwald GS. Species differences in egg transport in response to exogenous estrogen. *Anat Rec*. 1967;**157**(2):163–172.
35. Akison LK, Boden MJ, Kennaway DJ, Russell DL, Robker RL. Progesterone receptor-dependent regulation of genes in the oviducts of female mice. *Physiol Genomics*. 2014;**46**(16):583–592.
36. Tibbetts TA, Mendoza-Meneses M, O'Malley BW, Conneely OM. Mutual and intercompartmental regulation of estrogen receptor and progesterone receptor expression in the mouse uterus. *Biol Reprod*. 1998;**59**(5):1143–1152.
37. Couse JF, Yates MM, Sanford R, Nyska A, Nilson JH, Korach KS. Formation of cystic ovarian follicles associated with elevated luteinizing hormone requires estrogen receptor-beta. *Endocrinology*. 2004;**145**(10):4693–4702.
38. Couse JF, Bunch DO, Lindzey J, Schomberg DW, Korach KS. Prevention of the polycystic ovarian phenotype and characterization of ovulatory capacity in the estrogen receptor-alpha knockout mouse. *Endocrinology*. 1999;**140**(12):5855–5865.
39. Bridges PJ, Koo Y, Kang DW, et al. Generation of Cyp17iCre transgenic mice and their application to conditionally delete estrogen receptor alpha (Esr1) from the ovary and testis. *Genesis*. 2008;**46**(9):499–505.
40. Khan KS, Wojdyla D, Say L, Gülmezoglu AM, Van Look PF. WHO analysis of causes of maternal death: a systematic review. *Lancet*. 2006;**367**(9516):1066–1074.
41. Corpa JM. Ectopic pregnancy in animals and humans. *Reproduction*. 2006;**131**(4):631–640.
42. Horne AW, King AE, Shaw E, et al. Attenuated sex steroid receptor expression in fallopian tube of women with ectopic pregnancy. *J Clin Endocrinol Metab*. 2009;**94**(12):5146–5154.
43. Ulziibat S, Ejima K, Shibata Y, et al. Identification of estrogen receptor beta-positive intraepithelial lymphocytes and their possible roles in normal and tubal pregnancy oviducts. *Hum Reprod*. 2006;**21**(9):2281–2289.